Steel and Composite Structures, *Vol. 32, No. 5 (2019) 643-655*
DOI: https://doi.org/10.12989/scs.2019.32.5.643

On forced and free vibrations of cutout squared beams

Khalid H. Almitani [1a], Alaa A. Abdelrahman [2b] and Mohamed A. Eltaher[*1,2]

[1] *Mechanical Engineering Department, Faculty of Engineering, King Abdulaziz University, P.O. Box 80204, Jeddah, Saudi Arabia*
[2] *Mechanical Design & Production Department, Faculty of Engineering, Zagazig University, P.O. Box 44519, Zagazig, Egypt*

(*Received April 16, 2019, Revised July 18, 2019, Accepted August 4, 2019*)

Abstract. Perforation and cutouts of structures are compulsory in some modern applications such as in heat exchangers, nuclear power plants, filtration and microeletromicanical system (MEMS). This perforation complicates dynamic analyses of these structures. Thus, this work tends to introduce semi-analytical model capable of investigating the dynamic performance of perforated beam structure under free and forced conditions, for the first time. Closed forms for the equivalent geometrical and material characteristics of the regular square perforated beam regular square, are presented. The governing dynamical equation of motion is derived based on Euler-Bernoulli kinematic displacement. Closed forms for resonant frequencies, corresponding Eigen-mode functions and forced vibration time responses are derived. The proposed analytical procedure is proved and compared with both analytical and numerical analyses and good agreement is noticed. Parametric studies are conducted to illustrate effects of filling ratio and the number of holes on the free vibration characteristic, and forced vibration response of perforated beams. The obtained results are supportive in mechanical design of large devices and small systems (MEMS) based on perforated structure.

Keywords: free vibration; forced vibration; dynamical behavior; perforation; Euler-Bernoulli beam; semi-analytical method

1. Introduction

Most of engineering structures are subjected to vibrations due to the applied loads and the surrounding excitations. Safe and reliable design of these systems requires accurate analysis of their dynamical behaviors, such as, internal characteristics (natural frequencies) and overall behaviors (responses). Beam structure considered as a one of the most essential structures used widely in modern applications, ranging from large systems (i.e., aerospace, civil, marine, mechanical and nuclear structures), to microsystems (i.e., actuators, resonators, microphone, switches, and RF MEMS) to nanosystems (i.e., atomic force microscope, nanoprobes, nanoactuators, nanosensors, and nanoswitches).

Generally, perforated/cutouts structures are manufactured by etching number of identical holes in periodically in the structure. In most applications, these holes are circular or square holes and arranged in one or more rows. Perforation, in many large structures, is a necessary design feature due to technological reasons, such as, in the heat exchangers and nuclear power plants applications (Jeong and Amabili 2006), in ships and offshore structures, (Kim *et al*. 2015). In micro/nano-structures, perforation is often necessary for sacrificial-layer removal, representing a technological constraint for the designer, De Pasquale *et al*. (2010). The perforated beam and plates of MEMS are used to reduce the gas forces of oscillating structures, the squeeze film damping, and increase the switching speed, Rebeiz (2003). Further analysis reveals that perforated structure improves the switching time of the switch and also affects the capacitance of the switch, Bendali *et al*. (2006).

There is great difference between behavior and performance of perforated structures and fully ones. Duncan and Upfold (1965) obtained the equivalent elastic properties of bars and plates perforated on a square, a square-diagonal or a triangular pitch to model heat exchanger tube-plates. Yettram and Brown (1985) examined stability of flat square plates with central square perforations by a direct matrix method. In 1986, Brown and Yettram adopted previous model to investigate the stability of square perforated plates under combinations of bending, shear and direct load. Pedersen *et al*. (1996) predicted the in plane stiffness behavior and resonance frequency of beam-based micro-electromechanical resonant sensors by using finite difference method. Shanmugam *et al*. (1999) studied post-buckling behavior and the ultimate load capacity of perforated plates with different boundary conditions and subjected to uniaxial or biaxial compression using the finite element method. Jeong *et al*. (2001) performed an experimental modal analysis for perforated plates in contact with a fluid and showed that the natural frequencies of the clamped perforated plates in air could be predicted by using the equivalent elastic properties. Srivastava *et al*. (2003)

*Corresponding author, Professor,
E-mail: meltaher@kau.edu.sa;
mmeltaher@zu.edu.eg
[a] Ph.D., E-mail: kalmettani@kau.edu.sa
[b] Ph.D., E-mail: alaa.ahmed@zu.edu.eg;
alaaabouahmed@gmail.com

http://www.techno-press.org/?journal=scs&subpage=6
ISSN: 1229-9367 (Print), 1598-6233 (Online)

used finite element method to illustrate the vibration characteristics of stiffened plate with a cutout subjected to in-plane forces. Berggren *et al*. (2003) modeled the properties of regularly periodic holed structures materials by equivalent anisotropic materials and, concluded that, the equivalent anisotropic materials approaches are sophisticated and do not results in simple closed expressions for the structure resonance frequency.

Rastgoo *et al*. (2006) presented periodic solution for equation of motion of thick beams having arbitrary cross section with tip mass under harmonic support motion. Chen and Liu (2006) studied free and forced vibrations of a tapered cantilever beam carrying multiple point masses. Jeong and Amabili (2006) studied natural frequencies and the corresponding mode shapes of perforated beams, whose lower surfaces contacted with an ideal liquid by using Rayleigh–Ritz method. They reported that as the hole size increased the natural frequencies are gradually reduced while the effect of the hole shape on the natural frequencies is negligible for beam in air. Patel *et al*. (2010) investigated the effect of non-uniform in-plane pulsating edge loading on dynamic instability behavior of perforated stiffened shell panels. Cheng and Zhao (2010) focused on the cutout-strengthening of perforated plates subjected to uniaxial compressive loads. The square plates considered each has a centrally placed circular hole and four simply supported edges in the out-of-plane direction. Mali and Singru (2013) studied analytically the vibration of perforated rectangular plates with circular holes. They considered perforated plate as plate with uniformly distributed mass and their holes as concentrated negative masses. Mali and Singru (2015) derived an expression for the modal constant of the fundamental frequency of the perforated plate using Rayleigh's formulation. The fundamental frequency values were taken from experimental analysis. Kim *et al*. (2015) studied effect of reinforcement on buckling and ultimate strength of perforated plates.

Lee (2016) illustrated the effect of leakage on the sound absorption of a nonlinear perforated panel backed by a cavity. Mohammadimehr and Alimirzaei (2016) investigated nonlinear static and vibration of Euler-Bernoulli composite beam model reinforced by FG-SWCNT with initial geometrical imperfection using FEM. Akbarzade and Farshidianfar (2017) applied five different analytical methods to solve the dynamic model of the nonlinear oscillation equation of restrained cantilever tapered beam. Yuan *et al*. (2017) investigated distortional buckling of perforated cold-formed steel channel-section beams with circular holes in web. Zidi *et al*. (2017) proposed a novel simple higher-order shear deformation theory for bending and free vibration analysis of functionally graded (FG) beams. Benguediab *et al*. (2017) constructed an analytical solution of a plane stress problem for a cantilever beam made of a functionally graded material subjected to uniform loading.

Abdelbari *et al*. (2018) presented Single variable shear deformation model for bending analysis of thick beams. Heidari *et al*. (2018) developed numerical study for vibration response of concrete beams reinforced by nanoparticles. Yahiaoui *et al*. (2018) presented the role of micromechanical models in the mechanical response of elastic foundation FG sandwich thick beams. Loughlan and Hussain (2018) examined the response of simply supported steel plate shear webs with stiffened centrally located circular cut-outs when subjected to in-plane shear loading. Wang *et al*. (2018) investigated the buckling behavior of graphene platelets reinforced composite cylindrical shells with cutouts via finite element simulation. She *et al*. (2018a) studied thermal buckling and post-buckling behaviors of FGM tubes resting on elastic foundations. Based on Reddy's higher order shear deformation beam theory, She *et al*. (2018b) predicted wave propagation behaviors of functionally graded porous nanobeams (FGPNB). She *et al*. (2019a) extended their work in 2018 to investigate the snap-buckling behaviors of functionally graded (FG) porous curved nanobeams resting on elastic foundations for different boundary conditions. She *et al*. (2019b) investigated hygro-thermal wave propagation in functionally graded double-layered nanotubes systems.

Mechanical behaviors of perforated beam-based MEMS and NEMS devices and sensors have been studied by many researchers. De Pasquale *et al*. (2010) studied dynamic behavior and quality factors of oscillating perforated plates under the effect of squeeze film damping by both experimental and Multiphysics FEM simulations. Abbasnejad and Rezazadeh (2012) studied the mechanical behavior of a FGM micro-beam subjected to a nonlinear electrostatic pressure. Luschi and Pieri (2012) introduced closed forms for equivalent bending stiffness in the filled and the perforated sections of perforated beam to examine bending properties of beams with regular rectangular perforations. Tu *et al*. (2013) presented effects of etching holes on complementary metal oxide semiconductor–capacitive structure by the use of ANSYS simulation. Bouremana *et al*. (2013) presented a new first-order shear deformation beam theory based on neutral surface position for bending and free vibration analysis of functionally graded beams. Eltaher *et al*. (2013, 2014a, b) studied free vibration of thin and thick nanobeams by using finite element method. Luschi and Pieri (2014) presented closed expressions for geometrical properties of perforated beam with periodic square to investigate resonance frequencies of slender perforated beam. Sedighi *et al*. (2012) presented the advantages of different analytical techniques for the analysis of transverse vibration of cantilever beams. Based on the modified multilevel residue harmonic balance technique, Rahman *et al*. (2019) investigated the nonlinear forced vibration behavior of Euler Bernoulli beam resting on a nonlinear foundation. Applying the strain gradient elasticity theory, Sedighi (2014) studied the size dependent dynamic pull-in instability of vibrating micro actuated beams. Sedighi *et al*. (2015a) extended their work in 2014 to investigated the dynamic instability of double sided electromechanical nanosensors. Hieu and Hai (2019) applied the equivalent linearization technique with the weighted averaging method to study and analyze the nonlinear vibration behavior of Euler Bernoulli beams under axial loads. Mirzabeigy and Madoliat (2019) investigated the nonlinear free vibration behavior of double beam system considering inner layer nonlinearity.

Bennai *et al*. (2015) and Bourada *et al*. (2015) developed a new refined hyperbolic shear and normal deformation beam theory to study the free vibration and buckling of functionally graded (FG) sandwich beams. Eltaher *et al*. (2016) implemented higher-order shear deformation beam theories to investigate the effects of thermal load and shear force on the buckling of nanobeams. Guha *et al*. (2015) presented general analytical model of capacitance of non-uniform meander based RF MEMS shunt switch with perforated structure incorporating fringing field effects. Sedighi *et al*. (2015b) exhibited the effect of the amplitude of vibrations on the pull-in instability and nonlinear natural frequency of a double-sided actuated microswitch by using a nonlinear frequency amplitude relationship. Luschi and Pieri (2016) developed analytical models to determine the resonance frequency of Lamé-mode resonators with a square grid of square perforations. They confirmed their predictions by both experimental data and finite element method simulations.

Chen and Meguid (2017) investigated the dynamic behavior of a micro-resonator under various levels of Alternating Current (AC) voltage, without a biased Direct Current voltage. Guha *et al*. (2017, 2018) presented a new method for design, modelling and optimization of a uniform MEMS shunt capacitive switch with perforation on upper beam to improve the Pull-in Voltage performance. Static bending, stability and dynamical behaviors of perforated nonlocal nanobeams has been investigated by Eltaher *et al*. (2018a, b) by using both Euler-Bernoulli and Timoshenko beam theories. Driz *et al*. (2018) presented a novel higher shear deformation theory (HSDT) for bending, buckling and free vibration investigations of isotropic and functionally graded (FG) sandwich plates. Kerid *et al*. (2019) investigated the magnetic field, thermal loads and small scale effects on the dynamic behaviors of perforated nanobeams with periodic square networks.

So far, to the best of the authors' knowledge, there is no attempt to study free and forced vibration responses of perforated beams. Therefore, the aim of the present work is to present a detailed analytical and semi analytical methodologies capable of analyzing the free and forced vibration behaviors of perforated Euler Bernoulli beams (PEBB) for the first time. Through this study, simple mathematical expressions for natural frequencies, Eigen mode functions, and the forced vibration time response for a simply supported perforated Euler Bernoulli beam (PEBB) are derived. Semi-analytical mixed Galerkin Laplace technique is proposed. Numerical studies shows the significant effects of perforation (perforation size and number of cutouts) on the free and forced behaviors of perforated beam.

2. Theoretical aspects

In this section, the equivalent geometrical and material characteristics of the perforated beams are developed. Based on the Euler–Bernoulli beam theory (EBBT), the dynamic equation of motion of simply supported perorated beam with the associated boundary and initial conditions are presented.

2.1 Equivalent properties of perforated beam

Perforated beam is a type of periodic structures constructed by repeating a basic geometric unit to form a regular pattern. Perforated structure could be analyzed efficiently when the structure periodicity is considered. By considering the hole periodicity of the structure, the effective geometrical and material characteristics should be determined.

Considering a perforated beam, shown in Fig. 1, has a total length L, thickness h, width w, with a squared holes perforation pattern with spatial period l_s , side l_s -t_s, and a number of holes along the section is N. The ratio of the spatial period, t_s to the period length, l_s refers to the beam filling ratio, $\boldsymbol{\alpha}$ which can be expressed as follows

$$\alpha = \frac{t_s}{l_s} \qquad 0 \leq \alpha \leq 1, \qquad \alpha = \begin{cases} 0 & \text{Fully perforated} \\ 1 & \text{Fully filled} \end{cases} \tag{1}$$

Assume that the total stress along the cross section is the same for both complete beam and perforated one. Moreover, linear continuous stress distribution in the filled segments is also assumed. Under these assumption, following the procedure presented in Luschi and Pieri (2014), the equivalent bending stiffness can be expressed as

$$(EI)_{eq} = EI \left\{ \frac{\alpha(N+1)(N^2+2N+\alpha^2)}{(1-\alpha^2+\alpha^3)N^3+3\alpha N^2 +(3+2\alpha-3\alpha^2+\alpha^3)\alpha^2 N+\alpha^3} \right\} \tag{2}$$

where, E is the elasticity modulus of the fully filled beam material, I is the second moment of area of the fully filled beam, N is the nuber of holes along the cross section, α is the filling ratio.

The equivalent mass per unit length of the perforated beam can be also obtained by integrating over the beam segment, Eltaher *et al*. (2018b), as

$$(\rho A)_{eq} = \rho A \left\{ \frac{[1-N(\alpha-2)]\alpha}{N+\alpha} \right\} \tag{3}$$

where, ρ and A are the mass density and the cross sectional area of the fully filled beam; respectively. It noticed from Eq. (3) that the relative mass per unit length increases with

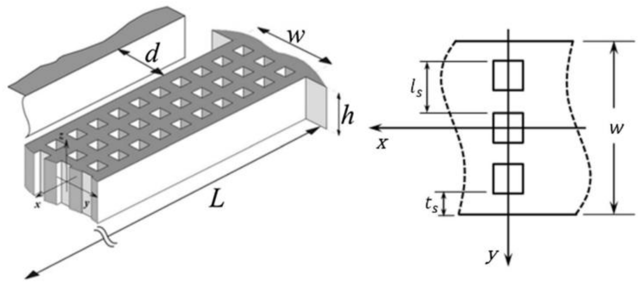

Fig. 1 Geometry of a perforated beam (Luschi and Pieri 2014)

increasing the beam filling ratio. On the other hand, it is slightly decreasing by increasing the number of holes at smaller values of the filling ratio. The equivalent rotary inertia of perforated beam can be obtained by integrating over a strip of N square cells of length ls, the equivalent moment of inertia per unit length can be expressed, as presented in Eltaher *et al*. (2018b), as

$$(\rho I)_{eq} = \rho I \left\{ \frac{\alpha \left[\begin{array}{c} (2-\alpha)N^3 + 3N^2 \\ -2(\alpha-3)(\alpha^2-\alpha+1)N + \alpha^2 + 1 \end{array} \right]}{(N+\alpha)^3} \right\} \tag{4}$$

2.2 Motion equations of perforated beams

According to the Euler–Bernoulli beam theory (EBBT), the rotation of the beam cross sections is neglected compared to the translation. Additionally, the angular distortion due to shear is neglected compared to the bending deformation. Based on EBBT, the displacement field can be expressed as

$$u = -z\frac{\partial w(x,t)}{\partial x}, \qquad v = 0, \qquad w = w(x,t) \tag{5}$$

where u, v, and w refer to the components of displacement in x, y, and z directions; respectively. The corresponding kinematic relations can be expressed as

$$\varepsilon_{xx} = \frac{\partial u}{\partial x} = -z\frac{\partial^2 w(x,t)}{\partial x^2} \tag{6}$$

Considering linear isotropic homogenous elastic materials, the constitutive law can be written as

$$\sigma_{xx} = -Ez\frac{\partial^2 w(x,t)}{\partial x^2} \tag{7}$$

The dynamic equation of motion with the associated boundary conditions can be obtained by applying the generalized Hamilton's principle as

$$\delta \int_{t_1}^{t_2} (\pi - T - W)\, dt = 0 \tag{8}$$

where π, T, and W are the strain energy, the kinetic energy, and the work done by the external forces of perforated beam; respectively. Eq. (8) can be expressed as, Rao (2007)

$$\begin{aligned} \delta \int_{t_1}^{t_2} \Bigg\{ & \frac{1}{2}\int_0^l (EI)_{eq}\left(\frac{\partial^2 w(x,t)}{\partial x^2}\right)^2 dx \\ & -\frac{1}{2}\left[\int_0^l (\rho I)_{eq}\left(\frac{\partial^3 w(x,t)}{\partial x^2 \partial t}\right)^2 dx \right. \\ & \left. + \int_0^l (\rho A)_{eq}\left(\frac{\partial w(x,t)}{\partial t}\right)^2 dx \right] \\ & - \int_0^l f(x,t)\, w(x,t) dx \Bigg\} dt = 0 \end{aligned} \tag{9}$$

Evaluating the integrals in Eq. (9), the dynamic equation of motion for perforated Euler Bernoulli beams [PEBB] can be written as

$$\begin{aligned} (\rho A)_{eq}\frac{\partial^2 w(x,t)}{\partial t^2} - (\rho I)_{eq}\frac{\partial^4 w(x,t)}{\partial x^2 \partial t^2} \\ +(EI)_{eq}\left(\frac{\partial^4 w(x,t)}{\partial x^4}\right) = f(x,t) \end{aligned} \tag{10}$$

3. Solution methodology

In this section closed forms for resonant frequencies, Eigen mode functions, and the forced vibration time response for a simply supported perforated Euler Bernoulli beam (PEBB) are derived.

3.1 Free vibration

Considering free vibration analysis, the governing equation of motion can be written as

$$\begin{aligned} (\rho A)_{eq}\frac{\partial^2 w(x,t)}{\partial t^2} - (\rho I)_{eq}\frac{\partial^4 w(x,t)}{\partial x^2 \partial t^2} \\ +(EI)_{eq}\left(\frac{\partial^4 w(x,t)}{\partial x^4}\right) = 0 \end{aligned} \tag{11}$$

The free vibration response can be expressed as

$$w(x,t) = W(x)\exp(i\omega t) \tag{12}$$

where $W(x)$ is the Eigen mode shape function (eigenvector) and ω is the natural frequency (eigenvalue) of vibration. Substitute Eq. (12) into Eq. (11) yields

$$\begin{aligned} \{(EI)_{eq}\, D^{(4)} + (\rho I)_{eq}\omega^2\, D^{(2)} \\ -\omega^2(\rho A)_{eq}\}W(x)\exp(i\omega t) = 0 \end{aligned} \tag{13}$$

The general solution of Eq. (13) can be written as

$$\begin{aligned} W(x) = C_1\cos(D_1 x) + C_2\sin(D_1 x) \\ +C_3\cosh(D_2 x) + C_4\sinh(D_2 x) \end{aligned} \tag{14}$$

Considering the simply supported beam, the following boundary conditions are imposed

$$\begin{aligned} W(x)|_{x=0} = W(x)|_{x=L} \\ = W''(x)|_{x=0} = W''(x)|_{x=L} = 0 \end{aligned} \tag{15}$$

Substituting with Eq. (15) into Eq. (14) and solving for the unknown constants, the natural frequency of PEBB can be expressed as

$$\omega_n^2 = \frac{\left(\frac{n\pi}{L}\right)^4 (EI)_{eq}}{(\rho A)_{eq} + (\rho I)_{eq}\left(\frac{n\pi}{L}\right)^2} \tag{16}$$

For fully filled beam, Eq. (16) can be written as

$$\omega_n^2 = \frac{\left(\frac{n\pi}{L}\right)^4 \left(\frac{EI}{\rho A}\right)}{1 + \left(\frac{I}{A}\right)\left(\frac{n\pi}{L}\right)^2} \tag{17}$$

which is the same as what had obtained by many authors; Rao (2007) and Inman (2014)

Then the associated Eigen functions for simply supported beam are given by

$$W_n(x) = C\, sin\left(\frac{n\pi x}{L}\right),\ \ n = 1, 2, 3, \dots\dots\dots\dots\infty \tag{18}$$

where C is an arbitrary constant, n is the vibration mode. Since the Eigen function is arbitrary, then it can be normalized so that

$$\int_0^l \left(1 + \left(\frac{(\rho I)_{eq}}{(\rho A)_{eq}}\right)\left(\frac{n\pi}{L}\right)^2\right)\left(W_n(x)\right)^2 dx = 1 \tag{19}$$

Substitute Eq. (18) into Eq. (19) and evaluating the integral, the normalized Eigen function can be expressed as

$$W_n(x) = \sqrt{\frac{2}{\left\{(\rho A)_{eq} + (\rho I)_{eq}\left(\frac{n\pi}{L}\right)^2\right\}L}}\ sin\left(\frac{n\pi x}{L}\right), \quad n = 1, 2, 3, \dots\dots\dots\dots\infty \tag{20}$$

For the fully filled beam, neglecting the rotary inertia effect, the normalized Eigen function can be expressed as

$$W_n(x) = \sqrt{\frac{2}{\rho AL}}\ \sin\left(\frac{n\pi x}{L}\right),\ \ n = 1, 2, 3, \dots\dots\dots\dots\infty \tag{21}$$

Eq. (21) is identical as what had obtained by Rao (2007) and Humar (2012).

3.2 Forced vibration response

Consider a simply supported beam with length, L, width, b and depth h. the beam is subjected to a uniformly distributed load with intensity $\bar{P}$. To solve the nonhomogeneous differential equation of motion presented by Eq. (10) with the associated boundary and initial conditions, mixed Galerkin - Laplace technique is adopted. In this procedure, the Galerkin technique is applied to detect the special dependency of the forced vibration response while the Laplace and inverse Laplace techniques are used to obtain the time dependency. To do this the forced response is expressed by a summation of two separate multiplied functions, the first function is a spatially dependent function while the second is a time dependent one. The transverse deflection function can be expressed in the form

$$w_n(x,t) = \sum_{j=1}^{n} T_j(t) W_j(x) \tag{22}$$

where $W_j(x)$ is the j-th shape functions which satisfy all the boundary conditions and $T_j(t)$ is the corresponding time dependent amplitudes which satisfy the initial conditions. For the spatial domain the Galerkin method will be used and then, the techniques of the Laplace transform is applied for the time domain. The shape functions are chosen to be linearly independent, orthonormal and must satisfy all boundary conditions for the convergence of Galerkin method, such that.

$$\int_0^L W_i(x) W_j(x) dx = \delta_{ij} \tag{23}$$

Where δ_{ij} is the kroners delta. Although w_n satisfies the boundary conditions, it generally, does not satisfy equation (10). Substitute Eq. (22) into (10) the residual function can be expressed as

$$\begin{aligned} \bar{R}_n(x,t) = {} & (\rho A)_{eq}\left(\sum_{i=1}^{n} \ddot{T}_i(t) W_i(x)\right) \\ & -(\rho I)_{eq}\left(\sum_{i=1}^{n} \ddot{T}_i(t) W_i^{(2)}(x)\right) \\ & +(EI)_{eq}\left(\sum_{i=1}^{n} T_i(t) W_i^{(4)}(x)\right) - \bar{P} \end{aligned} \tag{24}$$

The shape function that satisfies all boundary conditions and the orthogonality condition of simply supported beam can be expressed as

$$\begin{aligned} & W_i(x) = \sqrt{\frac{2}{L}} \sin\left(\frac{i\pi x}{l}\right), \\ & W_i^{(2)}(x) = -\left(\frac{i\pi}{l}\right)^2 W_i(x) = -\lambda_i W_i(x), \\ \text{and} \\ & W_i^{(4)}(x) = \left(\frac{i\pi}{l}\right)^4 W_i(x) \\ & = (\lambda_i)^2 W_i(x) \quad i = 1,2,.,n,\ \ \lambda_i = \left(\frac{i\pi}{l}\right)^2 \end{aligned} \tag{25}$$

The Galerkin method requires that the residual to be orthogonal to each of the chosen shape functions, so

$$\iint_\Omega \bar{R}_n(x,t) W_i(x) dx dt = 0\,, \quad i = 1,2,\dots.,n \tag{26}$$

Where Ω = [0, l]×[0, t]. This leads to n equations verified by the functions $T_j(t)$

$$\begin{aligned} \int_0^t \int_0^l \Bigg(& (\rho A)_{eq}\left(\sum_{i=1}^{n} \ddot{T}_j(t) W_j(x)\right) \\ & -(\rho I)_{eq}\left(\sum_{i=1}^{n} \ddot{T}_j(t) W_j^{(2)}(x)\right) \\ & +(EI)_{eq}\left(\sum_{i=1}^{n} T_j(t) W_j^{(4)}(x)\right)\Bigg) \\ & -\bar{P} W_i(x) dx dt = 0 \end{aligned} \tag{27}$$

Using Eq. (23), Eq. (27) can be rewritten as

$$\left[(\rho A)_{eq} + (\rho I)_{eq}(\lambda_j)\right]\ddot{T}_j(t) + (\lambda_j)^2 (EI)_{eq} T_j(t) \tag{28}$$

$$= \int_0^L \bar{P}\, W_j(x)dx = \bar{p}\left(\sqrt{\frac{2}{L}} \times \frac{L}{j\pi}\right)\left(1 - cos(j\pi)\right) \quad (28)$$

Using the Laplace transform techniques and the initial conditions

$$\left.\frac{d^k T_j(t)}{dt^k}\right|_{t=0} = \int_0^L \frac{\partial^k w(x,0)}{\partial t^k} W_j(x)dx, \quad k = 0, 1, 2, \ldots\ldots n \quad (29)$$

The functions $T_j(t)$ are determined to be independent of one another. Finally, an approximate value of the transverse deflection $w(x, t)$ will be found by Eq. (22).

4. Validation of the developed procedure

Within this section the validity of the developed analytical procedure for analyzing perforated beams is checked and compared. Firstly, the first lowest eight resonant frequencies of a simply supported solid beam are compared with the theoretical and numerical results presented in Jeong and Amabili (2006). Secondly, the dependency of the 1st resonant frequency of the perforated clamped- clamped beam on both the filling ratio and the number of holes is checked and compared with the obtained results by Luschi and Pieri (2012).

4.1 Validation of solid beam

To check the validity of the developed analytical procedure for analyzing solid beams, consider a simply supported solid beam having a length of L = 0.96 m, a width of w = 0.12 m and a thickness of h = 0.005 m. The beam is made of Aluminum whose elastic characteristics are E = 69 GPa, ν = 0.3, and ρ = 2700 kg/m^3. The resonant frequencies of the solid beam for the first lowest eighths modes were obtained by Jeong and Amabili (2006). The developed methodology is applied to detect the first lowest eights circular frequencies. The obtained natural frequencies are listed in Table 1. It is noticed almost identical values of the natural frequencies are obtained compared with that obtained by Jeong and Amabili (2006). Moreover good agreement is detected between the obtained natural frequencies of perforated beam by the developed analytical procedure and that obtained by Jeong and Amabili (2006) and ANSYS. Moreover, good agreement is detected between the obtained natural frequencies by the developed analytical procedure and those numerically obtained by ANSYS.

4.2 Validation of perforated beam

Consider a clamped-clamped perforated beam with the following geometrical characteristics: length, L = 1401.1 *um*, width w = 46.9 *um*, and thickness, h = 46.9 *um*. The beam is made of [110] single crystal Silicon with the following elastic characteristics are E = 169 GPa, ν = 0.046, and ρ = 2329 kg/m^3. The resonant circular frequencies of fixed perforated beams can be written as

Table 1 Natural frequencies for solid and perforated beam

Mode	Present	Jeong and Amabili (2006)	ANSYS
1	12.44	12.4	12.5
2	49.75	49.8	49.9
3	111.93	111.9	112.7
4	198.98	199.0	201.1
5	310.91	310.9	315.3
6	447.72	447.7	455.6
7	609.39	608.4	622.0
8	795.94	795.9	814.5

$$f_n = \frac{1}{2\pi}\left(\frac{\left(\frac{(2n+1)\pi}{2L}\right)^4 \left((EI)_{eq}\right)}{(\rho A)_{eq} + \left((\rho I)_{eq}\right)\left(\frac{n\pi}{L}\right)^2}\right)^{\left(\frac{1}{2}\right)}, \quad n = 1,2,\ldots\ldots \quad (30)$$

where Luschi and Pieri (2014) obtained an expression for the resonant frequencies of the same clamped- clamped perforated beam with no shear deformation as

$$f_n = \frac{1}{2\pi}\left(\frac{\left(Z_{n,cc}(0)\right)^4 \left((EI)_{eq}\right)}{(\rho A)_{eq} L^4}\right)^{(1/2)}, n = 1,2,\ldots\ldots \quad (31)$$

in which $Z_{n,cc}$ are rational functions interpolating the roots of the clamped–clamped eigenvalue. To check the validity of the developed procedure, the rotary inertia term in Eq. (30) is neglected and the obtained resonant frequencies are compared with that obtained from Eq. (31) using the given values of $Z_{n,cc}(0)$ in Luschi and Pieri (2014). Dependency of the lowest four resonant frequencies on the filling ratio at different number of holes for the present model and that obtained from Eq. (31) developed by Luschi and Pieri (2014) are illustrated in Fig. 2 has been achieved.

5. Numerical analysis

Consider a simply supported beam with L = 10 m, width b = 0.2 m, height h = 0.4 m, the moment of inertia I = (bh^3/12) = 10.6667 × 10^{-4} m^4. The beam is subjected to a uniformly distributed load of intensity 500 N/m, which is applied suddenly at t = 0 and then maintained constant. The material is taken to have the density of 7850 kg/m^3 and E= 200 GPa. Substituting with the geometrical and material characteristics Eq. (38) can be rewritten as

$$w_n(x,t) = \sum_{j=1}^{n}\left\{C_j \times \sqrt{\frac{2}{L}} \times \sin\left(\frac{i\pi x}{l}\right) \times \left(1 - cos\omega_j t\right)\right\} \quad (32a)$$

with

$$C_j = \frac{\bar{p} \times \sqrt{\frac{2}{L}}\left(\frac{L}{j\pi}\right)^5 \left[(-1)^{j+1} + 1\right]}{(EI)_{eq}}, \quad (32b)$$

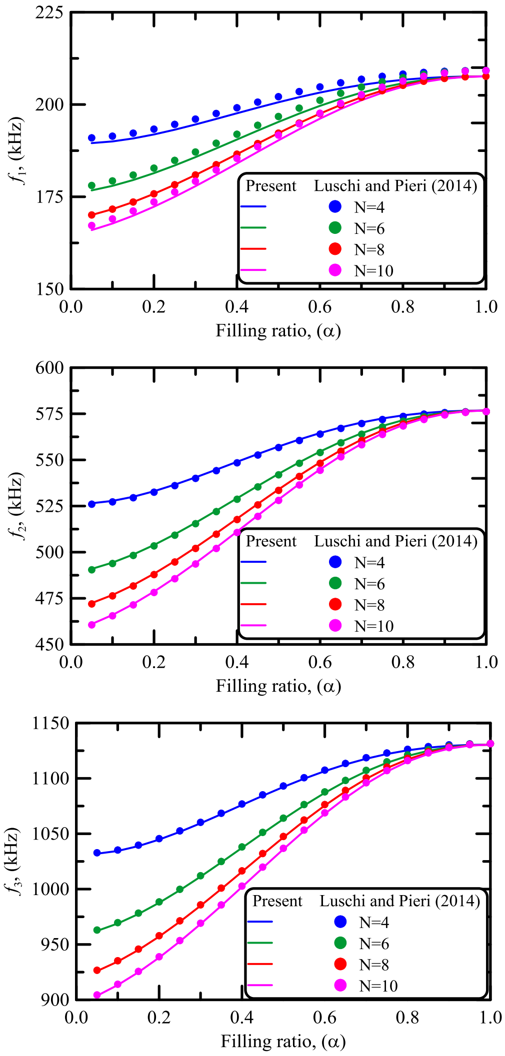

Fig. 2 Variation of the first three natural frequencies with the filling ratio at different number of holes

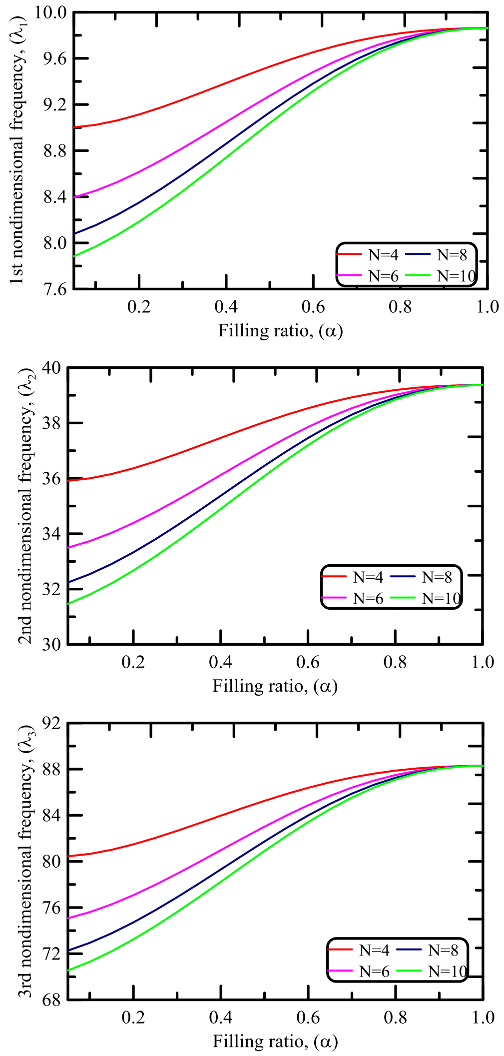

Fig. 3 Variation of the first three nondimensional natural frequencies (λ_i) with the filling ratio at different number of holes

$$\omega_j = \sqrt{\frac{\lambda_j^2 (EI)_{eq}}{(\rho A)_{eq} + \lambda_j (\rho I)_{eq}}}, \qquad \lambda_j = \left(\frac{j\pi}{L}\right)^2 \tag{32b}$$

In order to satisfy the dynamic equilibrium equation, a satisfactory number of terms should be considered in the closed form solution. Moreover, both the residual and the error percentage must be checked. Substitute Eq. (32a) into Eq. (24), the residual can be obtained. The relative error percentage can be expressed as

$$\%\,Error = \frac{\bar{R}_n(x,t)}{\bar{P}} \times 100 \tag{33}$$

In the following sections, effects of perforation process on the static deflection, resonant frequencies, mode shapes, and the transient vibration response are demonstrated.

5.1 Natural frequeies analysis

The nondimensional frequency of simply supported perforated beam can be written as

$$\lambda_n = \omega_n L^2 \sqrt{\frac{\rho A}{EI}}, \qquad \omega_n = \left(\frac{\left(\frac{n\pi}{L}\right)^4 \left((EI)_{eq}\right)}{(\rho A)_{eq} + \left((\rho I)_{eq}\right)\left(\frac{n\pi}{L}\right)^2}\right)^{\left(\frac{1}{2}\right)}, \qquad n = 1,2,\ldots\ldots \tag{34}$$

The dependencies of the lowest four resonant frequencies on both filling ratio and the number of holes are investigated.

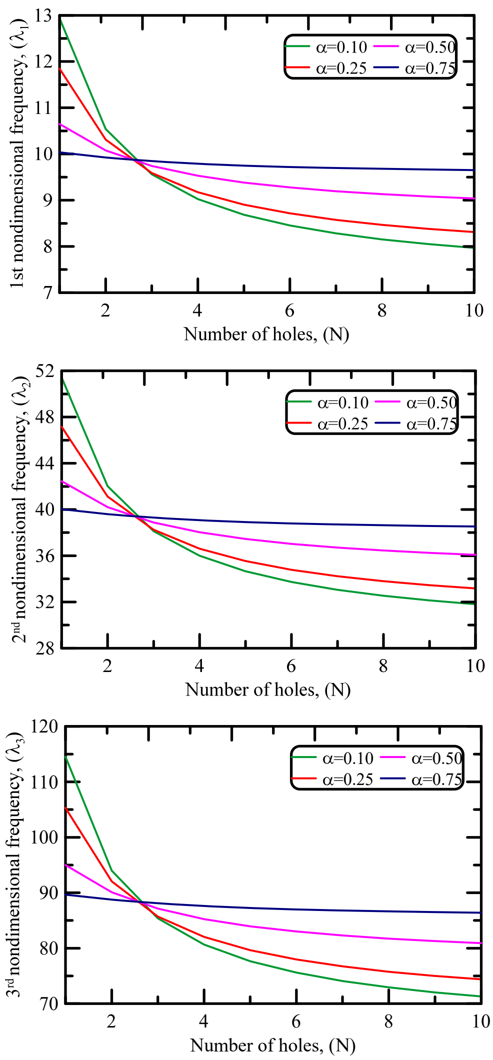

Fig. 4 Variation of the first three nondimensional natural frequencies (λ_i) with the number of holes at different filling ratios

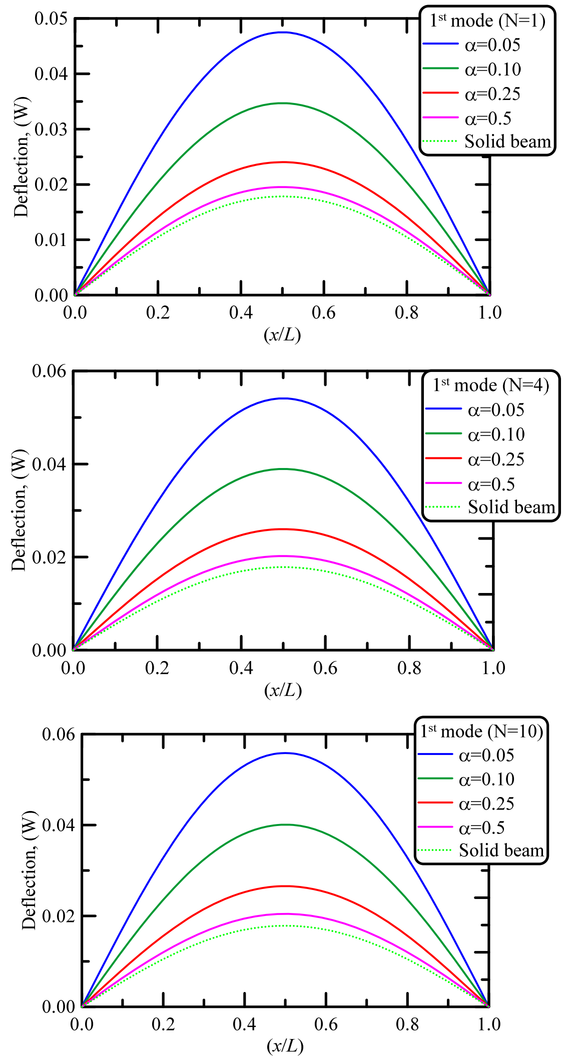

Fig. 5 Variation of 1st normalized mode shape at different filling ratios for N = 1, 4, and 10

a. Effect of filling ratio

Dependency of the resonant frequency on the filling ratio at different number of holes is depicted in Fig. 3. It is noticed that, for the considered number of holes, the lowest three resonant frequencies increase with increasing of the filling ratio. Moreover, for all values of N and $\alpha > 0.8$, all corresponding resonant frequencies are asymptotic to the corresponding resonant frequency of the fully filled solid beam.

b. Effect of number of holes

Variation of the resonant frequency with the number of holes at different filling ratios is depicted in Fig. 4. It is noticed that the natural frequencies are decreasing with increasing the number of holes, especially for all filling ratio values which are less than 0.75. For values of the filling ratio greater than 0.75, the rate of decreasing rate in the resonant frequencies is insignificant.

5.2 Mode shapes analysis

The normalized mode shapes of the perforated beam, $W_n(x)$ expressed by Eq. (20) is also affected by the perforation process. The dependency of the normalized mode shapes on both filling ratio and number of holes are presented below.

a. Effect of filling ratio

Variations of the first three mode shapes at different filling ratio for different values of the number of holes are depicted in Figs. 5-7. It is noticed that the perforation process has an insignificant effect on the location of nodes for all mode shapes. Only the amplitude of the normalized mode shapes is affected by the perforation process. Higher values for the amplitudes of the normalized mode shapes are detected for small filling ratios. As the filling ratio increases and approaches unity, the normalized mode shapes amplitudes approaches the amplitudes of the corresponding normalized mode shapes of the fully filled

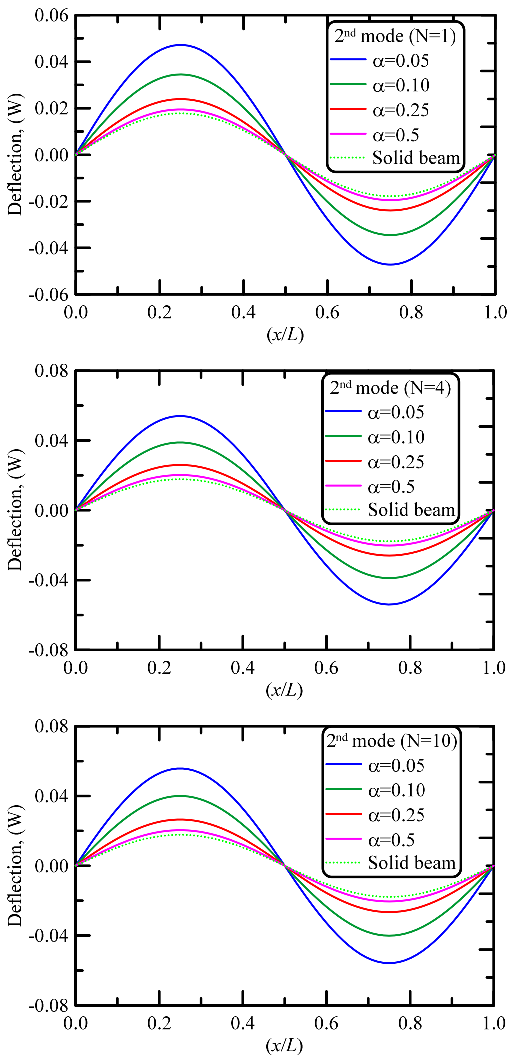

Fig. 6 Variation of 2nd normalized mode shape at different filling ratios for N = 1, 4, and 10

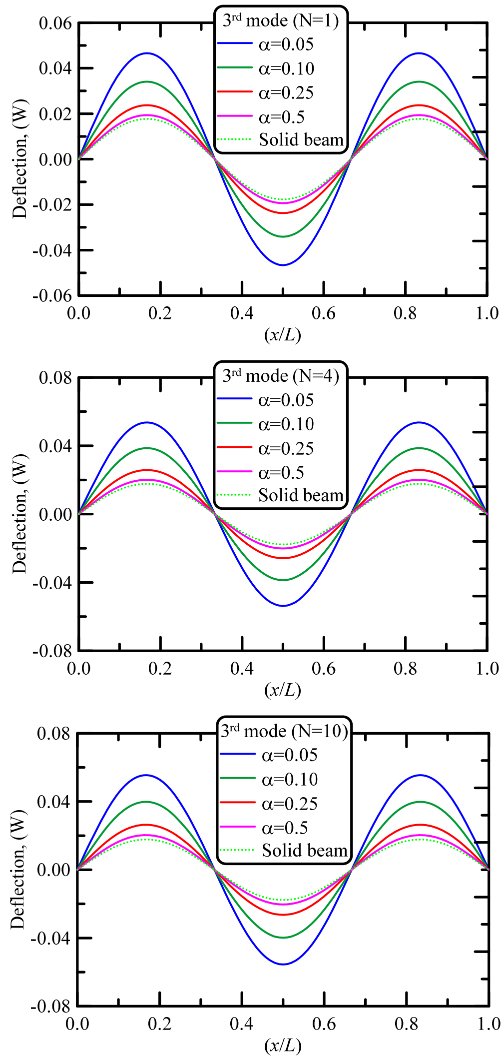

Fig. 7 Variation of 3rd normalized mode shape at different filling ratios for N = 1, 4, and 10

beam (solid beam). On the other hand, increasing the number of holes results in increases the amplitudes of the normalized mode shapes.

b. Effect number of holes

Dependency of the first three mode shapes on the number of holes at different filling ratios are shown in Figs. 8-10. It is noticed that the change in the amplitudes normalized mode shapes amplitudes is mainly associated with filling ratio of the perforated beam. At smaller values of the filling ratio, a noticeable increase in the normalized mode shapes amplitudes. On the other hand insignificant increase in the normalized mode shapes amplitudes is detected as the filling ratio exceeds 0.5.

5.3 Forced response

The forced vibration response of the perforated simply supported beam under uniformly distributed load of intensity 500 N/m is investigated. To attain equilibrium, the residual and consequently the relative error percentage should be as minimum as possible. The equilibrium equation is satisfied with the absolute relative error percentage of 0.0318%. As detected from Eq. (42a), the forced vibration response is dependent on the perforation process. Effects of both filling ratio and the number of holes on the transient vibration response are presented.

a. Effect of filling ratio

Variations of the maximum deflection of the perforated beam at different values of the filling ratio for different numbers of holes are depicted in Fig. 11. It can be detected that, the filling ratio has a significant effect on both amplitude and the phase shift of the forced vibration time response. Higher values of the amplitudes are detected at smaller values of the filling ratio. As the filling ratio increases, the amplitudes are decreased and the peak values of oscillations are shifted to right. For all values of $\alpha > 0.5$ he transient time response approaches that of the fully filled beam (solid beam at $\alpha = 1$).

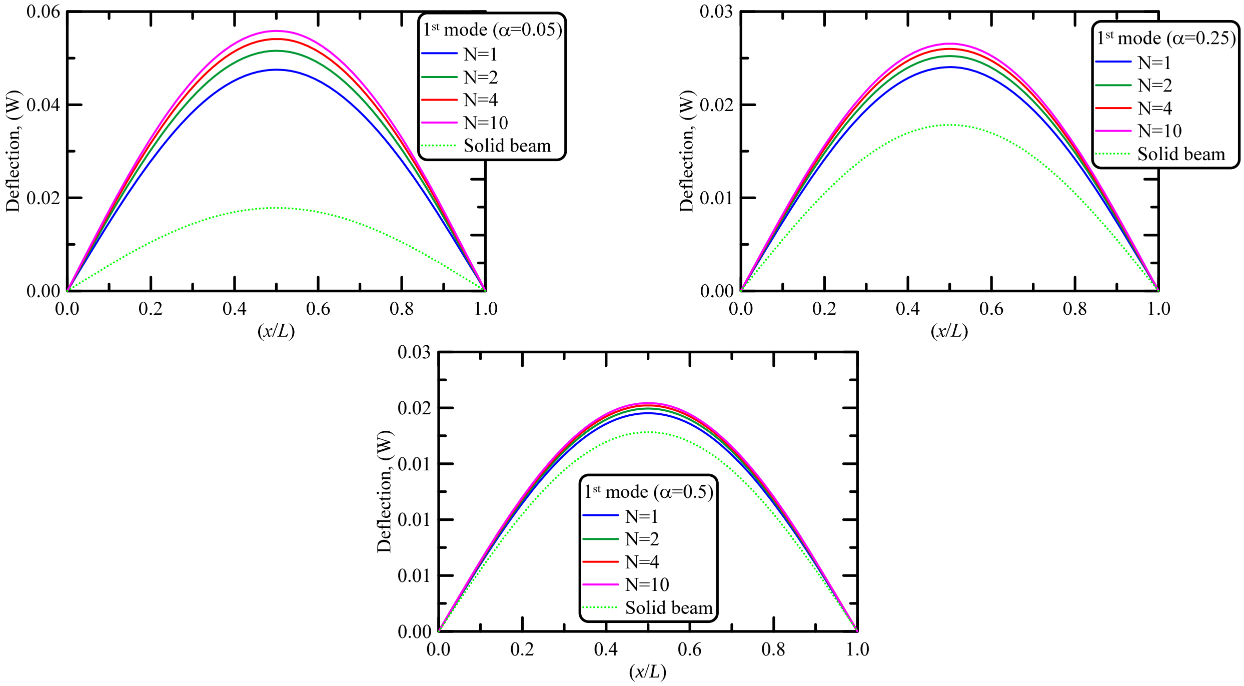

Fig. 8 Variation of 1st normalized mode shape at different hole numbers for α = 0.05, 0.25, and 0.5

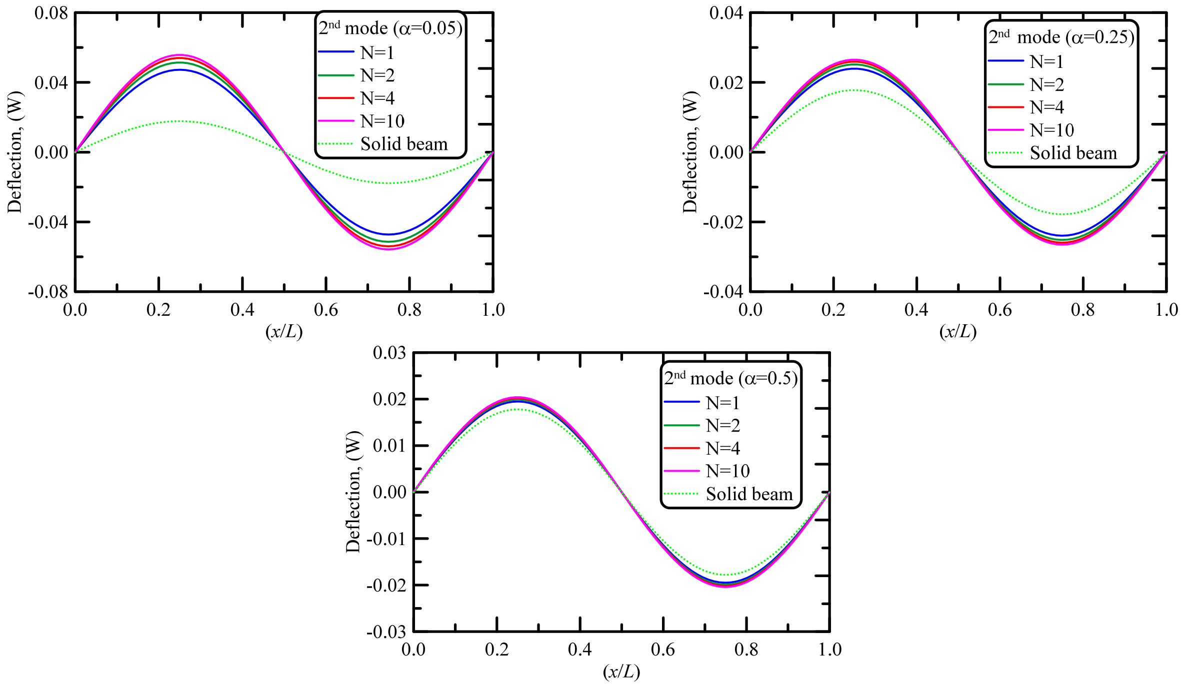

Fig. 9 Variation of 2nd normalized mode shape at different hole numbers for α = 0.05, 0.25, and 0.5

b. Effect of the number of holes

The dependency of the transient response of the perforated beam on the number of holes at different values of the filling ratio is illustrated in Fig. 12. It concluded that, variations of the amplitudes and phase shift of the forced vibration response with the number of holes are mainly dependent on the value of the beam filling ratio. Both amplitude and phase shift of the forced vibration response are increased with increasing the number of holes especially at smaller values of the filling ratio. The increasing rate of the forced vibration response with increasing the number of holes is decreased as the filling ratio increased. As the filling ratio approaches unity, the number of holes has insignificant effect on the transient vibration response of the perforated beam, as shown in Fig. 12.

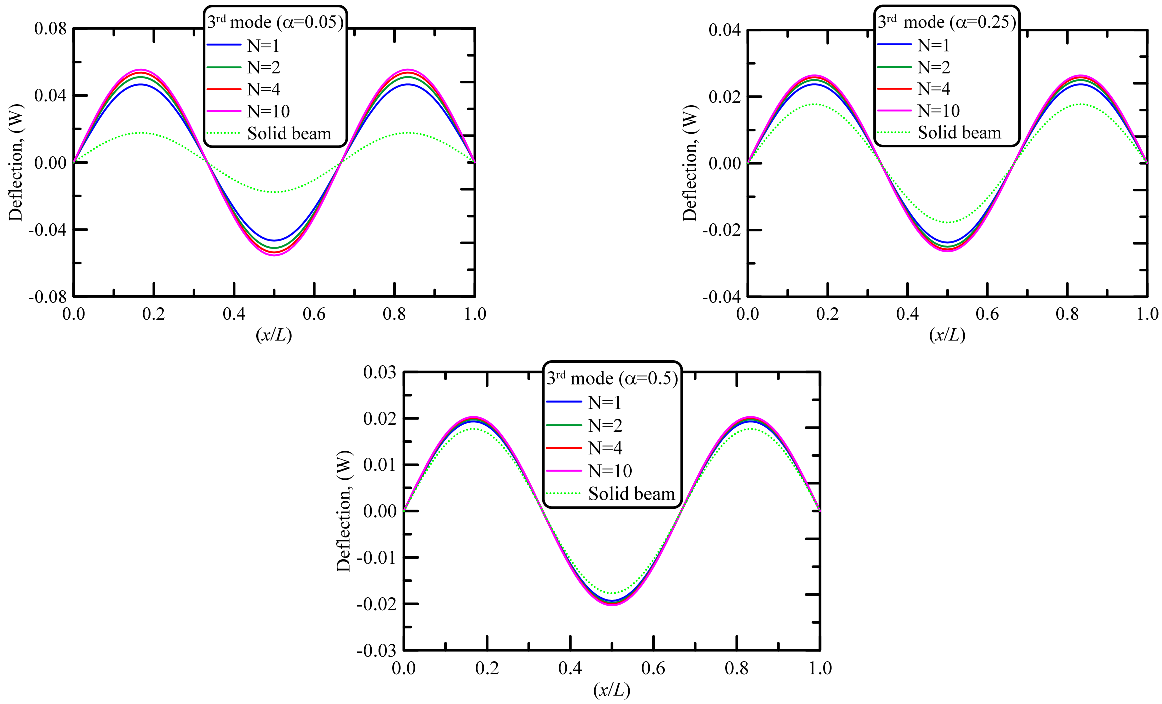

Fig. 10 Variation of 3rd normalized mode shape at different hole numbers for α = 0.05, 0.25, and 0.5

6. Conclusions

considered through perforation process. The developed analytical procedure is verified against both analytical and numerical analyses and good agreement is obtained. Parametric studies are conducted to illustrate the perforation effect on the free and forced vibration behavior of beams. The following concluding remarks are derived:

- Increasing the number of holes results in a decrease of the resonant frequencies. On the other hand, for the considered number of holes, the resonant frequencies are increased with increasing the filling ratio.
- Perforation process has no effect on locations of nodes in the mode shapes. The same locations of nodes are detected for all mode shapes as detected in the fully filled solid beam.
- Amplitudes of the mode shapes are highly affected by the filling ratio especially for $\alpha < 0.5$. As the filling ratio approaches unity, the amplitudes of the mode shapes approaches the corresponding amplitudes of the solid beam.
- At lower values of the filling ratio significant increase in the mode shape amplitude is detected. On the other hand for higher values of filing ratio $\alpha >$ 0.5, insignificant effect of the number of holes on the mode shapes is detected.
- The transient vibration effect is highly affected by the perforation process. The amplitude of the vibratory motion increases as the filling ratio decreases. As the filling ratio approaches unity, the time response of the perforated beam approaches that of the corresponding solid beam.
- As detected in mode shapes, the effect of the number of holes on the transient response is mainly on the value of the filling ratio.

Acknowledgments

This work was supported by the Deanship of Scientific Research (DSR), King Abdulaziz University, Jeddah, under Grant no. (D-043-135-1440). The authors, therefore, gratefully acknowledge the DSR technical and financial support.

References

Abbasnejad, B. and Rezazadeh, G. (2012), "Mechanical behavior of a FGM micro-beam subjected to a nonlinear electrostatic pressure", *Int. J. Mech. Mater. Des.*, **8**(4), 381-392. https://doi.org/10.1007/s10999-012-9202-x

Abdelbari, S., Amar, L.H.H., Kaci, A. and Tounsi, A. (2018), "Single variable shear deformation model for bending analysis of thick beams", *Struct. Eng. Mech., Int. J.*, **67**(3), 291-300. https://doi.org/10.12989/sem.2018.67.3.291

Akbarzade, M. and Farshidianfar, A. (2017), "Nonlinear dynamic analysis of an elastically restrained cantilever tapered beam", *J. Appl. Mech. Tech. Phys.*, **58**(3), 556-565. https://doi.org/10.1134/S002189441703021X

Bendali, A., Labedan, R., Domingue, F. and Nerguizian, V. (2006), May), "Holes effects on RF MEMS parallel membranes capacitors", *Proceedings of Canadian Conference on Electrical and Computer Engineering*, *CCECE'06*, Ottawa, Canada, May, pp. 2140-2143.

Benguediab, S., Tounsi, A., Abdelaziz, H.H. and Meziane, M.A.A. (2017), "Elasticity solution for a cantilever beam with exponentially varying properties", *J. Appl. Mech. Tech. Phys.*,

58(2), 354-361. https://doi.org/10.1134/S0021894417020213

Bennai, R., Atmane, H.A. and Tounsi, A. (2015), "A new higher-order shear and normal deformation theory for functionally graded sandwich beams", *Steel Compos. Struct., Int. J.*, **19**(3), 521-546. https://doi.org/10.12989/scs.2015.19.3.521

Berggren, S.A., Lukkassen, D., Meidell, A. and Simula, L. (2003), "Some methods for calculating stiffness properties of periodic structures", *Applicat. Math.*, **48**(2), 97-110. https://doi.org/10.1023/A:1026090026531

Bourada, M., Kaci, A., Houari, M.S.A. and Tounsi, A. (2015), "A new simple shear and normal deformations theory for functionally graded beams", *Steel Compos. Struct., Int. J.*, **18**(2), 409-423. https://doi.org/10.12989/scs.2015.18.2.409

Bouremana, M., Houari, M.S.A., Tounsi, A., Kaci, A. and Bedia, E.A.A. (2013), "A new first shear deformation beam theory based on neutral surface position for functionally graded beams", *Steel Compos. Struct., Int. J.*, **15**(5), 467-479. https://doi.org/10.12989/scs.2013.15.5.467

Brown, C.J. and Yettram, A.L. (1986), "The elastic stability of square perforated plates under combinations of bending, shear and direct load", *Thin-Wall. Struct.*, **4**(3), 239-246. https://doi.org/10.1016/0263-8231(86)90005-4

Chen, D.W. and Liu, T.L. (2006), "Free and forced vibrations of a tapered cantilever beam carrying multiple point masses", *Structural Engineering and Mechanics*, **23**(2), 209-216.

Chen, X. and Meguid, S.A. (2017), "Dynamic behavior of micro-resonator under alternating current voltage", *Int. J. Mech. Mater. Des.*, **13**(4), 481-497. https://doi.org/10.1007/s10999-016-9354-1

Cheng, B. and Zhao, J. (2010), "Strengthening of perforated plates under uniaxial compression: Buckling analysis", *Thin-Wall. Struct.*, **48**(12), 905-914. https://doi.org/10.1016/j.tws.2010.06.001

De Pasquale, G., Veijola, T. and Somà, A. (2010), "Modelling and validation of air damping in perforated gold and silicon MEMS plates", *J. Micromech. Microeng.*, **20**(1), 015010. https://doi.org/10.1088/0960-1317/20/1/015010

Driz, H., Benchohra, M., Bakora, A., Benachour, A., Tounsi, A. and Bedia, E.A.A. (2018), "A new and simple HSDT for isotropic and functionally graded sandwich plates", *Steel Compos. Struct., Int. J.*, **26**(4), 387-405. https://doi.org/10.12989/scs.2018.26.4.387

Duncan, J.P. and Upfold, R.W. (1963), "Equivalent elastic properties of perforated bars and plates", *J. Mech. Eng. Sci.*, **5**(1), 53-65. https://doi.org/10.1243/JMES_JOUR_1963_005_009_02

Eltaher, M.A., Alshorbagy, A.E. and Mahmoud, F.F. (2013), "Vibration analysis of Euler–Bernoulli nanobeams by using finite element method", *Appl. Math. Model.*, **37**(7), 4787-4797. https://doi.org/10.1016/j.apm.2012.10.016

Eltaher, M.A., Abdelrahman, A.A., Al-Nabawy, A., Khater, M. and Mansour, A. (2014a), "Vibration of nonlinear graduation of nano-Timoshenko beam considering the neutral axis position", *Appl. Math. Computat.*, **235**, 512-529. https://doi.org/10.1016/j.amc.2014.03.028

Eltaher, M.A., Hamed, M.A., Sadoun, A.M. and Mansour, A. (2014b), "Mechanical analysis of higher order gradient nanobeams", *Appl. Math. Computat.*, **229**, 260-272. https://doi.org/10.1016/j.amc.2013.12.076

Eltaher, M.A., Khater, M.E., Park, S., Abdel-Rahman, E. and Yavuz, M. (2016), "On the static stability of nonlocal nanobeams using higher-order beam theories", *Adv. Nano Res., Int. J.*, **4**(1), 51-64. https://doi.org/10.12989/anr.2016.4.1.051

Eltaher, M.A., Kabeel, A.M., Almitani, K.H. and Abdraboh, A.M. (2018a), "Static bending and buckling of perforated nonlocal size-dependent nanobeams", *Microsyst. Technolog.*, **24**(12), 4881-4893. https://doi.org/10.1007/s00542-018-3905-3

Eltaher, M.A., Abdraboh, A.M. and Almitani, K.H. (2018b), "Resonance frequencies of size dependent perforated nonlocal nanobeam", *Microsyst. Technol.*, **24**(9), 3925-3937. https://doi.org/10.1007/s00542-018-3910-6

Guha, K., Kumar, M., Agarwal, S. and Baishya, S. (2015), "A modified capacitance model of RF MEMS shunt switch incorporating fringing field effects of perforated beam", *Solid-State Electronics*, **114**, 35-42. https://doi.org/10.1016/j.sse.2015.07.008

Guha, K., Laskar, N.M., Gogoi, H.J., Borah, A.K., Baishnab, K.L. and Baishya, S. (2017), "Novel analytical model for optimizing the pull-in voltage in a flexured MEMS switch incorporating beam perforation effect", *Solid-State Electronics*, **137**, 85-94. https://doi.org/10.1016/j.sse.2017.08.007

Guha, K., Laskar, N.M., Gogoi, H.J., Baishnab, K.L. and Rao, K.S. (2018), "A new analytical model for switching time of a perforated MEMS switch", *Microsyst. Technol.*, 1-10. https://doi.org/10.1007/s00542-018-3803-8

Heidari, A., Keikha, R., Haghighi, M.S. and Hosseinabadi, H. (2018), "Numerical study for vibration response of concrete beams reinforced by nanoparticles", *Struct. Eng. Mech., Int. J.*, **67**(3), 311-316. https://doi.org/10.12989/sem.2018.67.3.311

Hieu, D. and Hai, N.Q. (2019), "Free vibration analysis of quintic nonlinear beams using equivalent linearization method with a weighted averaging", *J. Appl. Computat. Mech.*, **5**(1), 46-57. https://doi.org/10.22055/JACM.2018.24919.1217

Humar, J. (2012), *Dynamics of Structures*, CRC press.

Inman, D.J. (2014), *Engineering Vibration*, (4th Ed.), Pearson Education, Pearson, London, UK.

Jeong, K.H. and Amabili, M. (2006), "Bending vibration of perforated beams in contact with a liquid", *J. Sound Vib.*, **298**(1-2), 404-419. https://doi.org/10.1016/j.jsv.2006.05.029

Jeong, K.H., Ahn, B.K. and Lee, S.C. (2001), "Modal analysis of perforated rectangular plates in contact with water", *Struct. Eng. Mech., Int. J.*, **12**(2), 189-200. https://doi.org/10.12989/sem.2001.12.2.189

Kim, J.H., Jeon, J.H., Park, J.S., Seo, H.D., Ahn, H.J. and Lee, J.M. (2015), "Effect of reinforcement on buckling and ultimate strength of perforated plates", *Int. J. Mech. Sci.*, **92**, 194-205. https://doi.org/10.1016/j.ijmecsci.2014.12.016

Lee, Y.Y. (2016), "The effect of leakage on the sound absorption of a nonlinear perforated panel backed by a cavity", *Int. J. Mech. Sci.*, **107**, 242-252. https://doi.org/10.1016/j.ijmecsci.2016.01.019

Loughlan, J. and Hussain, N. (2018), "The post-buckled failure of steel thin plate shear webs with stiffened centrally located cut-outs", *Thin-Wall. Struct.*, **128**, 80-91. https://doi.org/10.1016/j.tws.2017.07.015

Luschi, L. and Pieri, F. (2012), "A simple analytical model for the resonance frequency of perforated beams", *Procedia Eng.*, **47**, 1093-1096. https://doi.org/10.1016/j.proeng.2012.09.341

Luschi, L. and Pieri, F. (2014), "An analytical model for the determination of resonance frequencies of perforated beams", *J. Micromech. Microeng.*, **24**(5), 055004. https://doi.org/10.1088/0960-1317/24/5/055004

Luschi, L. and Pieri, F. (2016), "An analytical model for the resonance frequency of square perforated Lamé-mode resonators", *Sensors Actuators B: Chem.*, **222**, 1233-1239. https://doi.org/10.1016/j.snb.2015.07.085

Mali, K.D. and Singru, P.M. (2013), "Determination of the fundamental frequency of perforated rectangular plates: Concentrated negative mass approach for the perforation", *Adv. Acoust. Vib.* http://dx.doi.org/10.1155/2013/972409

Mali, K.D. and Singru, P.M. (2015), "Determination of modal constant for fundamental frequency of perforated plate by Rayleigh's method using experimental values of natural frequency", *Int. J. Acoust. Vib.*, **20**(3), 177-184.

Mirzabeigy, A. and Madoliat, R. (2019), "A Note on Free Vibration of a Double-beam System with Nonlinear Elastic Inner Layer", *J. Appl. Computat. Mech.*, **5**(1), 174-180. https://doi.org/10.22055/JACM.2018.25143.1232

Mohammadimehr, M. and Alimirzaei, S. (2016), "Nonlinear static and vibration analysis of Euler-Bernoulli composite beam model reinforced by FG-SWCNT with initial geometrical imperfection using FEM", *Struct. Eng. Mech., Int. J.*, **59**(3), 431-454. https://doi.org/10.12989/sem.2016.59.3.431

Patel, S.N., Datta, P.K. and Sheikh, A.H. (2010), "Effect of harmonic in-plane edge loading on dynamic stability of stiffened shell panels with cutouts", *Int. J. Appl. Mech.*, **2**(4), 759-785. https://doi.org/10.1142/S1758825110000743

Pedersen, M., Olthuis, W. and Bergveld, P. (1996), "On the mechanical behaviour of thin perforated plates and their application in silicon condenser microphones", *Sensors Actuators A: Phys.*, **54**(1-3), 499-504. https://doi.org/10.1016/S0924-4247(95)01189-7

Kerid, R., Bourouina, H., Yahiaoui, R., Bounekhla, M. and Aissat, A. (2019), "Magnetic field effect on nonlocal resonance frequencies of structure-based filter with periodic square holes network", *Physica E: Low-dimens. Syst. Nanostruct.*, **105**, 83-89. https://doi.org/10.1016/j.physe.2018.05.021

Rahman, M., Hasan, A.S. and Yeasmin, I.A. (2019), "Modified Multi-level Residue Harmonic Balance Method for Solving Nonlinear Vibration Problem of Beam Resting on Nonlinear Elastic Foundation", *J. Appl. Computat. Mech.*, **5**(4), 627-638. https://doi.org/10.22055/JACM.2018.26729.1352

Rao, S.S. (2007), *Vibration of Continuous Systems*, John Wiley & Sons.

Rastgoo, A., Ebrahimi, F. and Dizaji, A.F. (2006), "On the existence of periodic solution for equation of motion of thick beams having arbitrary cross section with tip mass under harmonic support motion", *Int. J. Mech. Mater. Des.*, **3**(1), 29-38. https://doi.org/10.1007/s10999-006-9011-1

Rebeiz, G.M. (2004), *RF MEMS: Theory, Design, and Technology*, John Wiley & Sons.

Sedighi, H.M. (2014), "Size-dependent dynamic pull-in instability of vibrating electrically actuated microbeams based on the strain gradient elasticity theory", *Acta Astronautica*, **95**, 111-123. https://doi.org/10.1016/j.actaastro.2013.10.020

Sedighi, H.M., Shirazi, K.H. and Noghrehabadi, A. (2012), "Application of recent powerful analytical approaches on the non-linear vibration of cantilever beams", *Int. J. Nonlinear Sci. Numer. Simul.*, **13**(7-8), 487-494. https://doi.org/10.1515/ijnsns-2012-0030

Sedighi, H.M., Koochi, A., Daneshmand, F. and Abadyan, M. (2015a), "Non-linear dynamic instability of a double-sided nano-bridge considering centrifugal force and rarefied gas flow", *Int. J. Non-Linear Mech.*, **77**, 96-106. https://doi.org/10.1016/j.ijnonlinmec.2015.08.002

Sedighi, H.M., Shirazi, K.H. and Changizian, M. (2015b), "Effect of the amplitude of vibrations on the pull-in instability of double-sided actuated microswitch resonators", *J. Appl. Mech. Tech. Phys.*, **56**(2), 304-312. https://doi.org/10.1134/S0021894415020169

Shanmugam, N.E., Thevendran, V. and Tan, Y.H. (1999), "Design formula for axially compressed perforated plates", *Thin-Wall. Struct.*, **34**(1), 1-20. https://doi.org/10.1016/S0263-8231(98)00052-4

She, G.L., Ren, Y.R., Xiao, W.S. and Liu, H.B. (2018a), "Study on thermal buckling and post-buckling behaviors of FGM tubes resting on elastic foundations", *Struct. Eng. Mech., Int. J.*, **66**(6), 729-736. https://doi.org/10.12989/sem.2018.66.6.729

She, G.L., Yan, K.M., Zhang, Y.L., Liu, H.B. and Ren, Y.R. (2018b), "Wave propagation of functionally graded porous nanobeams based on non-local strain gradient theory", *Eur. Phys. J. Plus*, **133**(9), 368. https://doi.org/10.1140/epjp/i2018-12196-5

She, G.L., Ren, Y.R. and Yan, K.M. (2019a), "On snap-buckling of porous FG curved nanobeams", *Acta Astronautica*, **161**, 475-484. https://doi.org/10.1016/j.actaastro.2019.04.010

She, G.L., Ren, Y.R. and Yan, K.M. (2019b), "Hygro-thermal wave propagation in functionally graded double-layered nanotubes systems", *Steel Compos. Struct., Int. J.*, **31**(6), 641-653. https://doi.org/10.12989/scs.2019.31.6.641

Srivastava, A.K.L., Datta, P.K. and Sheikh, A.H. (2003), "Prediction of Natural Frequencies of Stiffened Plates with Cutouts Subjected to In-plane Forces", In: *Structural Stability And Dynamics*: With CD-ROM (Volume 1), pp. 278-282. https://doi.org/10.1142/9789812776228_0036

Tu, W.H., Chu, W.C., Lee, C.K., Chang, P.Z. and Hu, Y.C. (2013), "Effects of etching holes on complementary metal oxide semiconductor–microelectromechanical systems capacitive structure", *J. Intel. Mater. Syst. Struct.*, **24**(3), 310-317. https://doi.org/10.1177/1045389X12449917

Wang, Y., Feng, C., Zhao, Z. and Yang, J. (2018), "Buckling of graphene platelet reinforced composite cylindrical shell with cutout", *Int. J. Struct. Stabil. Dyn.*, **18**(3), 1850040. https://doi.org/10.1142/S0219455418500402

Yahiaoui, M., Tounsi, A., Fahsi, B., Bouiadjra, R.B. and Benyoucef, S. (2018), "The role of micromechanical models in the mechanical response of elastic foundation FG sandwich thick beams", *Struct. Eng. Mech., Int. J.*, **68**(1), 53-66. https://doi.org/10.12989/sem.2018.68.1.053

Yettram, A.L. and Brown, C.J. (1985), "The elastic stability of square perforated plates", *Comput. Struct.*, **21**(6), 1267-1272. https://doi.org/10.1016/0045-7949(85)90180-4

Yuan, W.B., Yu, N.T. and Li, L.Y. (2017), "Distortional buckling of perforated cold-formed steel channel-section beams with circular holes in web", *Int. J. Mech. Sci.*, **126**, 255-260. https://doi.org/10.1016/j.ijmecsci.2017.04.001

Zidi, M., Houari, M.S.A., Tounsi, A., Bessaim, A. and Mahmoud, S.R. (2017), "A novel simple two-unknown hyperbolic shear deformation theory for functionally graded beams", *Struct. Eng. Mech., Int. J.*, **64**(2), 145-153. https://doi.org/10.12989/sem.2017.64.2.145

Rebeiz, G.M. (2004), *RF MEMS: Theory, Design, and Technology*, John Wiley & Sons.

Duncan, J.P. and Upfold, R.W. (1963), "Equivalent elastic properties of perforated bars and plates", *J. Mech. Eng. Sci.*, **5**(1), 53-65. https://doi.org/10.1243/JMES_JOUR_1963_005_009_02

CC